

Flow Distribution in Manifolds

Asst. Prof. Dr. J. M. Hassan

*Mechanical Engineering Dept., College of Eng.
University of Technology, Baghdad, Iraq*

Dr. Abdulwahhab AbdulRazzaq

*Mechanical Engineering Dept., College of Eng.
Al-Mustansiriya University, Baghdad, Iraq*

Eng. B. K. Kamil

*M.Sc. in Mechanical Engineering
Al-Mustansiriya University, Baghdad, Iraq*

Abstract

A Numerical study of two-dimensional, turbulent, incompressible fluid flow through manifold pipe that divides flow to five consecutive laterals is carried out. Each lateral is oriented at ninety degree to manifold axis. The study is based on the solution of the elliptic partial differential equations representing the conservation of mass, momentum, turbulence energy and its dissipation rate in finite volume form. The turbulent viscosity and diffusion coefficients are calculated using the (k-ε) model. Different parameters are considered to illustrate their influences on the flow distribution along manifold. These parameters include the area ratio (the ratio of the sum of areas of all laterals to manifold area) (A.R), curvature radius at the junction points between manifold and laterals (R), and space between each two consecutive laterals.

The results show that the area ratio has a significant effect on flow distribution along manifold pipe and as a result of these effects the discharge through laterals near from uniform as the area ratio becomes less than unity ($A.R < 1$), while when area ratio becomes larger than unity ($A.R > 1$) the discharge distribution through laterals is far from uniform (flow rate through the last lateral will be greater than the flow through the first lateral), especially for short manifold ($L/D \leq 10$) and sharp-edged laterals. The value of skin friction factor will be decreased as area ratio becomes larger than unity. The rounding of lateral entrance, the variation in flow distribution is much greater, whereas the discharge will be increased at last two lateral pipes. The value of skin friction factor at wall of manifold decrease as curvature radius increases.

Finally as the space between each two consecutive laterals increases, the variation in discharge distribution through laterals decreases slowly.

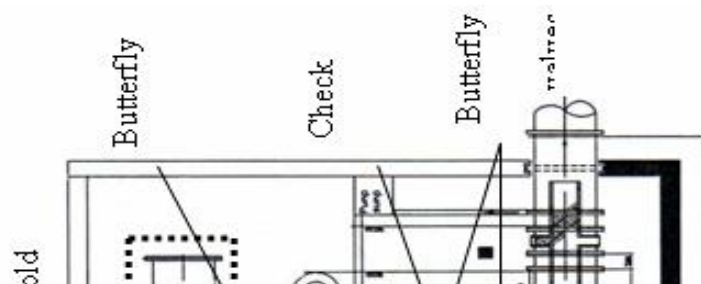
الخلاصة

تتضمن الدراسة الحاسوبية الحالية محاكاة الجريان المضطرب، ثنائي الأبعاد، اللانضغاطي داخل بوب متفرع، والذي يوزع الجريان إلى خمسة أنابيب جانبية متتالية ذات طول قصير. كل أنبوب جانبي يتقاطع مع إحدائيات الأنبوب المنوع بزوايا قائمة (٩٠ درجة). تتضمن الدراسة حل المعادلات التفاضلية الجزئية الاهليجية والمتمثلة بحفظ الكتلة، الزخم، الطاقة المضطربة ومعدل ضياعها، باستخدام الحجوم المحددة، ولقد حلت هذه المعادلات سوية مع الصيغ الجبرية للزوجة المضطربة ومعدل الانتشارية بوجود نظام الاضطراب المسمى $(k-\epsilon)$. وقد تم توضيح تأثير عدة عوامل هندسية على توزيع الجريان خلال الأنبوب المتفرع، وهذه العوامل تضمنت نسبة المساحة (مجموع مساحات الفروع مقسومة على مساحة الأنبوب الرئيسي)، نصف قطر التقوس، والمسافة بين الأنابيب الفرعية. نتائج هذه الدراسة أوضحت أن نسبة المساحة تملك تأثير ملموس وواضح على توزيع الجريان، ونسبة إلى هذا التأثير فإن التصريف خلال الأنابيب الفرعية سوف يقترب من التوزيع المنتظم عندما تكون نسبة المساحة أقل من واحد، بينما عندما تكون نسبة المساحة أكبر من واحد، فإن توزيع التصريف خلال الأنابيب الجانبية يبتعد من التوزيع المنتظم، وبالأخص إذا كان الأنبوب المنوع قصير ($L/D \leq 10$). قيمة الاحتكاك عند جدار الأنبوب المنوع سوف يقل عندما تكون نسبة المساحة أكبر من واحد. عندما يكون مدخل الأنبوب منحنى، فإن الفرق في توزيع الجريان خلال التفرعات الجانبية سوف يزداد، وخصوصاً سوف يتركز التصريف في آخر تفرعين جانبيين. أخيراً عندما تزداد المسافة بين الأنابيب الفرعية، فإن الفرق في توزيع التصريف خلال الأنابيب الجانبية سوف يقل ببطء.

1. Introduction

Dividing flow takes place in a manifold that distributes a fluid flow uniformly to a series of successive lateral outlet ports. The fluid flow through manifolds has many applications, such as; flow distribution systems in treatment plants that treat water and wastewater, the piping system of pumping stations that involves a main supply manifold with many side branches to pumps, and in irrigation systems. The function of a pumping station is to transfer water from a source to a required destination such as supplying water to the distribution networks. The water pumping station consists of pumps, pipes of various sizes, valves, pipe fittings, and distribution reservoirs...etc. pumps which pumped water directly into transmission lines, and distribution system. Pipes are divided into two types: in the first, suction and discharge piping of pumps. In the second, supply and collecting manifolds, these pipes carry water from reservoir to each part in pumping station. Valves are used to control the flow of water through the pipes ^[1].

Rasafa pumping station for reservoir No-3 has been chosen in this study to analyze water distribution through the supply manifold and its laterals, as shown at dotted lines in **Fig.(1)**. Rasafa pumping station consists of ten centrifugal vertical split case pumps connected in parallel joint together into supply manifold (header) in order to feed those pumps. Eight of those have high flow (800 l/sec), and two of them have low flow (500 l/sec), whereas the total flow becomes (7400 l/sec). This pump station contains one butterfly valve before each pump and two butterfly valves with check valve after each pump.



In practical cases, there is a strong inter-linkage between flow distribution and manifold design, which is determined by the area ratio (AR) (the ratio of the sum of areas of all laterals to manifold area), curvature radius (R) and the space between each two consecutive laterals

(1).with this perspective, various aspects of this problem have been studied by a number of investigators. Keller ^[2] presented a study that deals with the general problem of manifolds supplying fluids to a set of parallel pipes or ducts, or discharging through a numerous opening distributed along the manifold length. For this case of the problem, the fundamental equation relating pressure and flow to position along the manifold is reduced to a second-order differential equation for which no solution has been found. Therefore, a point-by-point numerical method was used, starting with unit velocity and pressure at the discharge lateral nearest the dead end of the manifold and working back from lateral to lateral toward the inlet end. Bajura ^[3] developed analytical procedure for determining the performance of dividing-flow type of manifolds in which the lateral tubes form sharp-edged junctions at right angles to the manifold axis. A mathematical model describing the flow behavior at discrete branch point was formulated in terms of momentum balance along the manifold pipe.

Hudson et. al. ^[4] presented a simplified approach based on successive-approximations scheme for predicting the hydraulic behavior of manifold pipe that divides flow to five consecutive short length laterals. In the first stage, the head losses are calculated by assuming equal flow distribution between laterals. In the second stage, better estimation of the lateral flow distribution along the manifold can be made using the previous head loss results. In their study, a series of mathematical iterations may be used to predict the flow distribution.

Hayes et. al. ^[5] studied the laminar flow characteristics of a Newtonian, incompressible fluid in a two-dimensional, planar, right angled tee branch over a range of inlet Reynolds number of (10-800) by solving the Navier-Stokes equations using a finite element discretization. Neary et. al. ^[6] developed numerical model for predicting a three-dimensional, steady, turbulent flows through lateral intakes for rectangular T-junctions. The flow field was discretized using Reynolds-averaged Navier-stokes equations closed with the isotropic (k-ε) turbulence model of Wilcox on a non-staggered mesh by using a finite difference formulas.

The main objective of the present investigation is to predicate the effect of changing the area ratio (AR), curvature radius at the junction point between manifold and lateral (R), and the space between each two consecutive laterals (l), on flow distribution along manifold pipe that divides flow to five consecutive short length laterals. Each lateral is oriented at ninety degree to manifold axis and in square-edged, uniform spacing between laterals.

2. Mathematical Formulation

Governing Equations

The flow is assumed to be two dimensional, steady, incompressible and constant laminar viscosities. Therefore, the mean flow is assumed to satisfy the incompressible Navier-Stokes equations with an eddy viscosity. A set of the differential equations which are commonly used to depict the flow under prescribed conditions can be presented in a general form.

$$\frac{\partial}{\partial x}(\rho u \phi) + \frac{\partial}{\partial y}(\rho v \phi) = \frac{\partial}{\partial x} \left(\Gamma_{\phi} \frac{\partial \phi}{\partial x} \right) + \frac{\partial}{\partial y} \left(\Gamma_{\phi} \frac{\partial \phi}{\partial y} \right) + S_{x,y} \dots\dots\dots (1)$$

Equation (1) is called the general transport equation. The argument ϕ identifies the dependent variable, Γ is the diffusion coefficient for variable ϕ . The two terms on the left-hand side are the convective terms; the first two terms on the right-hand side are the diffusive term, and the last term is the source term. The source term includes both the source of ϕ and any other terms that cannot find place in any of the convection or diffusion terms. The governing differential equations in engineering problems are generally derived in Cartesian (i.e. rectangular) coordinate systems. Finite difference methods for solving differential equations require that continuous physical space is to be discretized into a uniform orthogonal computational space.

Difficulties associated with the use of Cartesian coordinate system motivate the introduction of a transformation from physical (x, y) space to a generalized curvilinear coordinate (ξ, η) space. The final complete transformed form of the conservative general transport equation for property ϕ can be written, as follows:

$$\frac{\partial}{\partial \xi}(\rho G1\phi) + \frac{\partial}{\partial \eta}(\rho G2\phi) = \frac{\partial}{\partial \xi} (J\Gamma_{\phi}\phi_{\xi}a1) + \frac{\partial}{\partial \eta} (J\Gamma_{\phi}\phi_{\eta}a2) + S_{total} \dots\dots\dots (2)$$

where:

S_{total} : represents the total source term

$$S_{total} = JS_{x,y} + S_{\xi,\eta} \dots\dots\dots (3)$$

3. Discretization Method

The finite-volume method of Patankar [7] will be used for the discretization of the conservative form of the governing equations. The calculations domain is divided into a number of non-overlapping control volumes surrounding each grid point **Fig.(2)**. Then, the governing equations can be integrated over discrete control volume in the computational space. Final discretized algebraic equation for property ϕ is given by the following:

$$A_P \phi_P = \sum A_{nb} \phi_{nb} + \bar{S}_{total} \Delta V \dots\dots\dots (4)$$

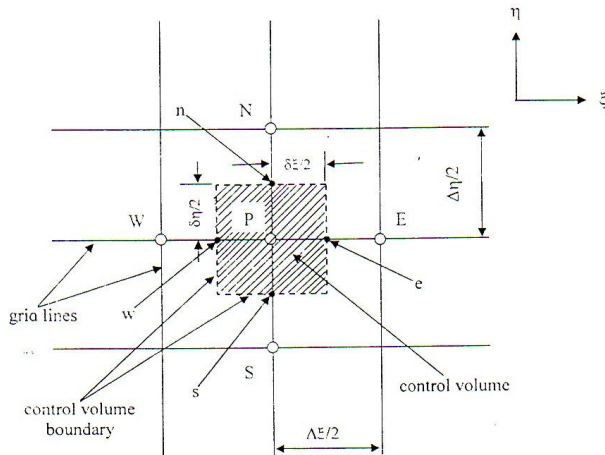


Figure (2) Control volume arrangement for general variable

The boundary conditions that required for the solution of equation (4) as shown below Fig. (3).

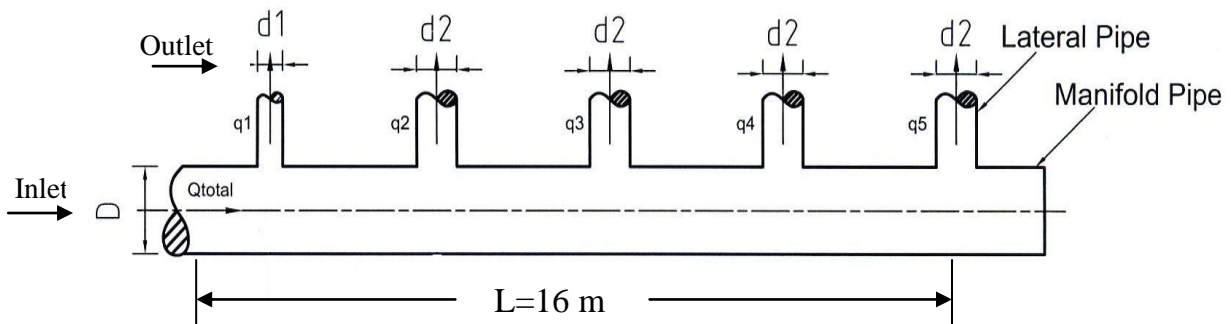


Figure (3) Two-dimensional manifold geometry

1. Inlet boundary condition. The distribution of all flow variables are specified at inlet boundaries (the line $I=1$ or $i=2$ for u_ξ velocity). An approximation for the inlet distribution for k and ϵ as given below:

$$k = \frac{2}{3} (\mathbf{u}_{\xi_{in}} T_i)^2 \dots\dots\dots (5)$$

$$\epsilon = C_\mu^{3/4} \frac{k^{3/2}}{\ell} \dots\dots\dots (6)$$

$$\ell = 0.07L \dots\dots\dots (7)$$

where:

L : is equivalent hydraulic diameter,

C_μ : is a universal constant, 0.09,

ℓ : is the length scale of turbulence and

T_i : turbulence intensity.

2. Outlet Boundary Conditions. The gradient of all variables at the outlet are specified equal to zero.

3. Wall Boundary Conditions. The optimum near wall relationships for the standard k-ε model from extensive computing trials Versteeg and Malalasekera [8], are implemented as follows.

✚ Momentum equation tangential to wall

Wall shear stress:

$$\tau_w = \rho C_\mu^{1/4} K_P^{1/2} u_P / u^+ \dots\dots\dots (8)$$

Wall force:

$$F_s = -\tau_w A_{cell} = -(\rho C_\mu^{1/4} K_P^{1/2} u_P / u^+) A_{cell} \dots\dots\dots (9)$$

✚ Momentum equation normal to wall

Normal velocity =0

✚ Turbulent kinetic energy equation

$$\text{Net-k source per unit volume} = (\tau_w u_P - \rho C_\mu^{1/4} K_P^{3/2} u^+) \Delta \nabla / \Delta y_P \dots\dots\dots (10)$$

✚ Dissipation rate equation

Set nodal value:

$$\epsilon_P = C_\mu^{3/4} K_P^{3/2} / (K \Delta y_P) \dots\dots\dots (11)$$

where:

A_{cell} : is the wall area of control volume.

These relationships should be used in conjunction with universal velocity (u^+) for near wall turbulent flows:

$$u^+ = \frac{1}{\kappa} \ln(Ey^+) \dots\dots\dots (12)$$

The SIMPLE algorithm of Patankar and Spalding [9], is adopted in this current work. The governing equation was solved using upwind differences scheme, and the solution is repeated until convergences achieved.

4. Result and Discussion

4-1 Manifold Geometry

The geometry under consideration is a short manifold pipe ($L/D \leq 10$) of Al-Rasafa pumping station that divides flow to five consecutive laterals. Each lateral is oriented at ninety degrees to the manifold and is square-edged. At the inlet of manifold, the flow rate is taken as ($Q=3.7 \text{ m}^3/\text{sec}$) and has dead end, as shown in **Fig.(3)**.

Owing to the complex geometry of the manifold, the computational grid should be selected carefully so that it could be dense in a region where high gradients occur and/or near the wall boundary. The grid is generated by solving an elliptic partial differential equations, where the numerical computation is performed on ($222*50$) grid nodes in x and y directions respectively.

4-2 Influence of Area Ratio

The influence of area ratio, can be divided into three cases, and for each case different diameters of manifold ($D=1400, 1600, 1800\text{mm}$) and for laterals ($d=500,750,800,900 \text{ mm}$) have been examined to predict their effect on flow distribution along the manifold pipe. The flow distribution for different cases analysis is as follows:

✚ Case 1

Figures (4) and (5) show the streamlines contour and velocity vectors of flow through manifold pipe for different area ratios ($A.R=0.6, 1.4, 1.6, 2$), by keeping the manifold diameter constant ($D=1400\text{mm}$) and different diameters of lateral pipes ($d=500,750,800,900\text{mm}$) respectively. It becomes obvious from **Fig.(4)**, that one recirculation zone can be seen clearly at left wall of each lateral pipe (from first to fourth lateral), while the recirculation zone of the last lateral is formed at the right wall, and one recirculation zone will be formed at the junction point between manifold and Last lateral pipe. The size of the lateral recirculation zones will be decreased along the manifold pipe. It is well evident that the increase in area ratio (from 0.6 to 2), produces an increase in the size of lateral recirculation zones.

Figure (6) shows the pressure distribution along manifold pipe. It can be seen that the pressure increase along the center-line of manifold pipe.

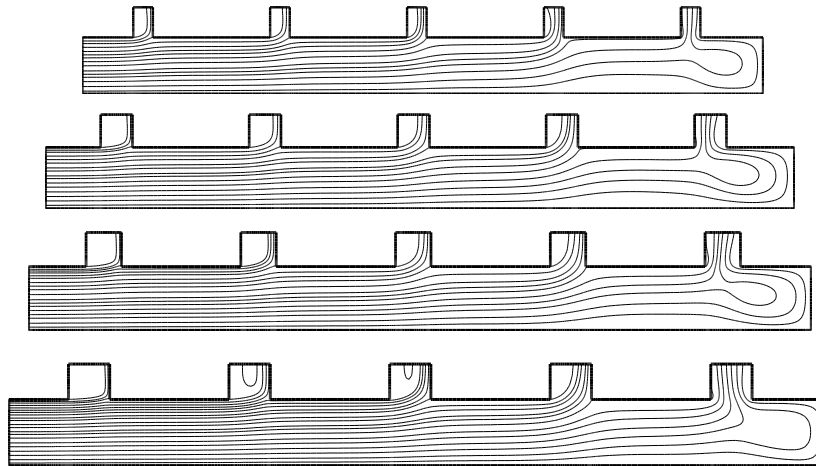


Figure (4) Contours of streamline for manifold of diameter $D=1400\text{mm}$, and lateral diameters ($d=500,750,800,900\text{mm}$), $R=0.0001\text{m}$

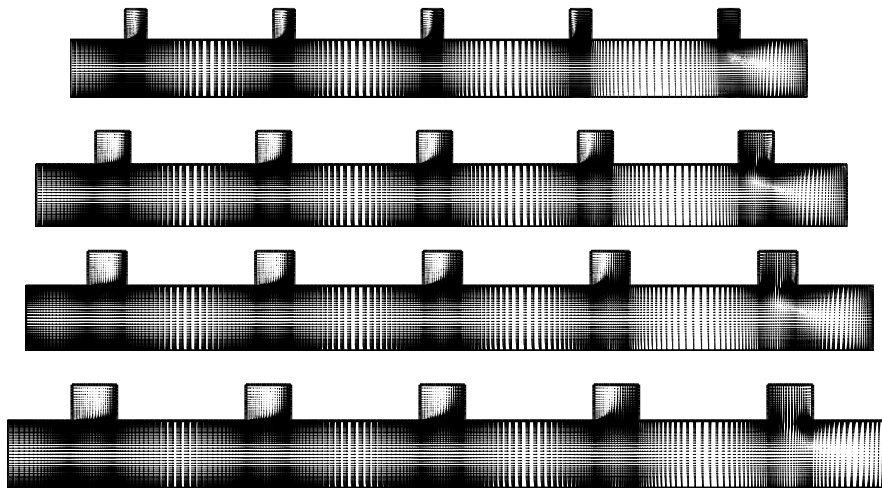


Figure (5) Velocity vectors for manifold of diameter $D=1400\text{mm}$, and lateral diameters ($d=500,750,800,900\text{mm}$) respectively, $R=0.0001\text{m}$

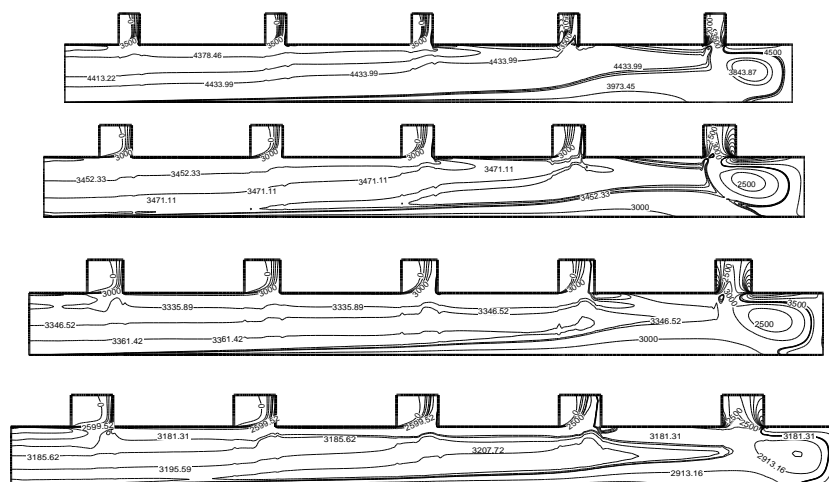


Figure (6) Pressure contours for manifold of diameter $D=1400\text{mm}$, and lateral diameters ($d=500,750,800,900\text{mm}$), $R=0.0001\text{m}$

From Fig.(7), it is noticed that the center-line velocity will decrease along manifold pipe due to the change in flow rate along the manifold pipe, and when area ratio increases (from 0.6 to 2), the center-line velocity of manifold increases in values (but decrease remains along manifold pipe), in accordance with Bernoulli's theorem. This tends to increase the fluid pressure along the manifold pipe.

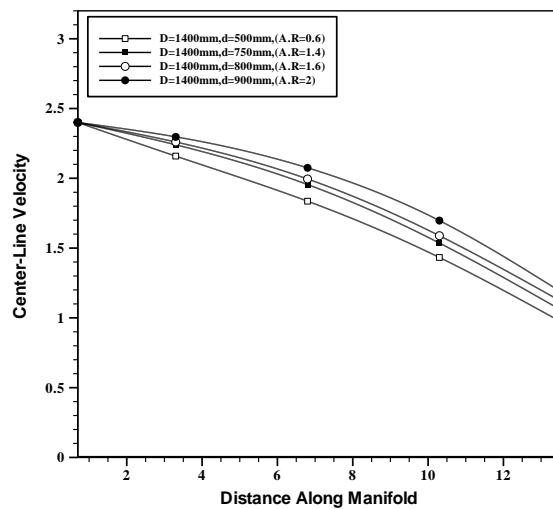


Figure (7) Velocity distribution at centerline of manifold for different area ratio

Figure (8) shows the predicted distribution of flow along manifold for different area ratios. The results show, at $A.R=0.6$, about 29.5% from total flow is discharged from last lateral pipe and about 10.5% from total flow is discharged from first lateral pipe. At $A.R=1.4$, about 35% from total flow is discharged from last lateral and 7.75% is discharged from first lateral pipe. At $A.R=1.6$, about 37.5% from total flow exit from last lateral and about 7% exit from first lateral, finally at $A.R=2$, 41.5% from total flow discharged from last lateral and 5.5% from first lateral. The disparities of flow distribution grow greater as the area ratio increase above unity ($A.R=1$). These predictions are very similar to those reported by Hudson H. E. et. al. [4].

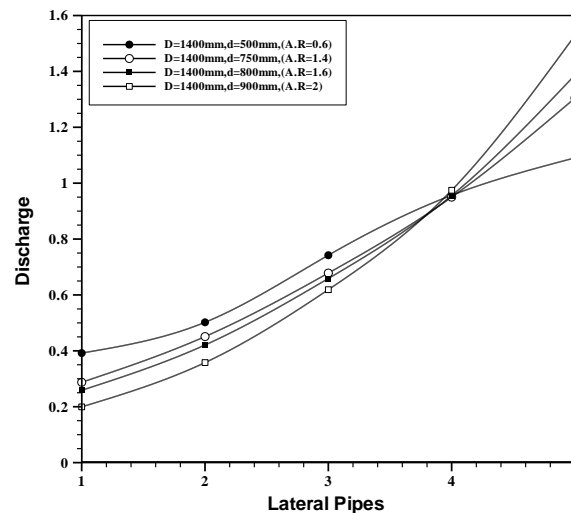


Figure (8) Discharge distribution along manifold length for different area ratio

Figure (9) illustrates the skin friction distribution at the wall of manifold pipe, where the maximum value of friction factor is ($C_f=0.011$) at $A.R=0.6$, finally, at $A.R=2$, the maximum value of friction factor is ($C_f=0.0095$), then it is found that the value of skin friction factor at the wall of manifold decreases as area ratio increases. Finally, for cases 2&3 we get, as area ratio decrease (less than unity), may help to make the flow distribution in lateral pipes as uniform as possible. In addition, the pressure will be increased along the centerline of the manifold pipe, and the value of friction factor decreases as area ratio increases.

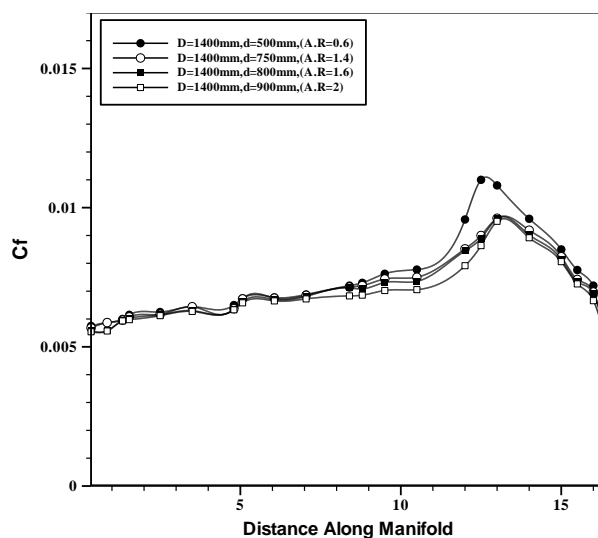


Figure (9) Skin friction distribution at wall of manifold for different area ratio

4-3 Influence of the Curvature Radius:

Figures (10 to 14) represent the effect of changing the curvature radius at the junction points on the properties and behavior of flow through manifold pipe, by taking different values of curvature radius ($R=50,150,250,400$ mm) respectively, with different area ratios ($A.R=0.85, 1, 1.25$). It is noticed that the recirculation zones in the last two lateral pipes disappear drastically as the curvature radius increases from (50 to 400mm), as shown in **Fig.(10)**. **Figure (11)** show the velocity vector of flow through manifold pipe for different

curvature radius. It can be seen from **Fig.(12)** that the centerline velocity will decrease along manifold pipe. It becomes obvious that the influence of this factor ($R=50,150,250,400$ mm) makes the flow distribution along the manifold pipe not uniform. This is noticeable by the fact the discharge increases along the manifold pipe, in addition to the rounding entrance of lateral pipes. At ($A.R=0.85, R=50\text{mm}$) about 32% from total flow is discharged from last lateral and 8.25% is discharged from first lateral, while at ($A.R=0.85, R=400\text{mm}$) about 39% is discharged from last lateral and about 3.5% is discharged from first lateral, the disparities increase as area ratio increase from (0.85 to 1.25) as shown in **Fig.(13)**. From **Fig.(14)**, it can be seen, the value of friction factor decreases as the curvature radius increases.

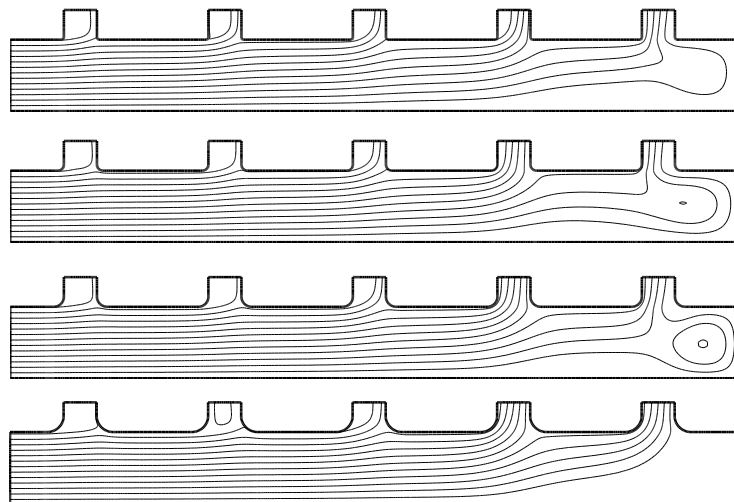


Figure (10) Contours of streamline for (A.R=0.85), with different curvature radius (R=50,150,250,400mm)

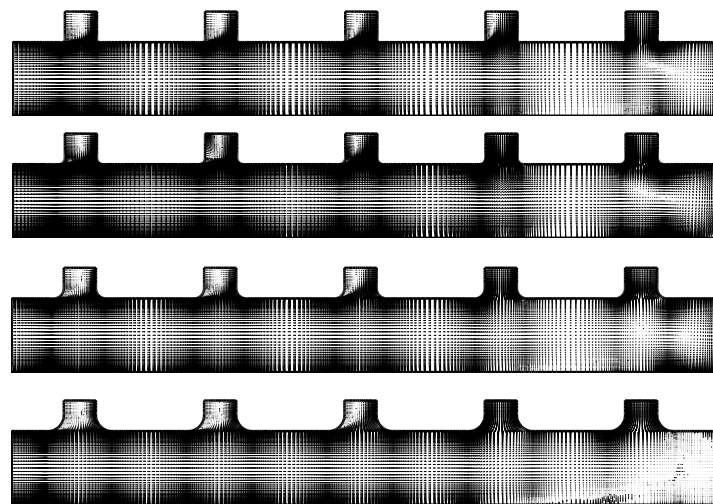


Figure (11) Velocity vectors for manifold of diameter $D=1800\text{mm}$, and lateral diameter $d=750\text{mm}$, with different curvature radius (R=50,150,250,400mm)

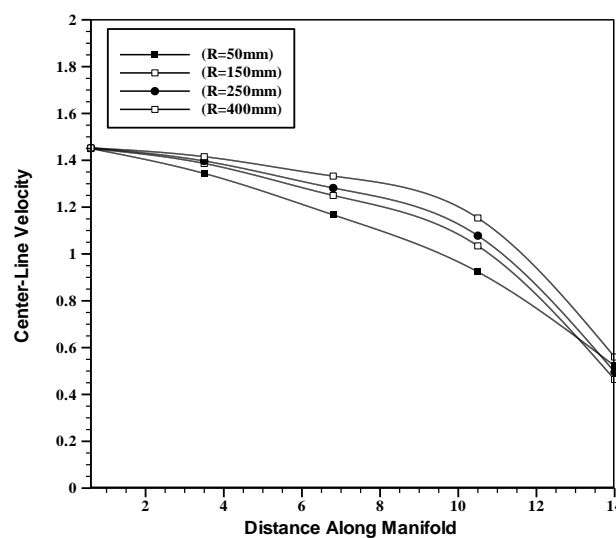


Figure (12) Velocity distribution at centerline for different curvature radius

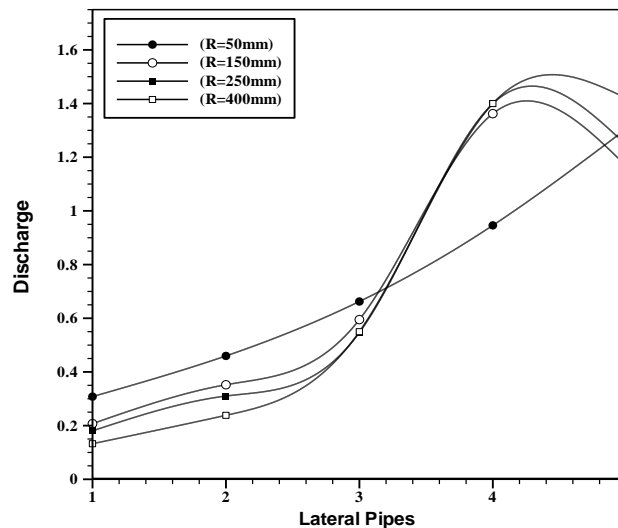


Figure (13) Discharge distribution along manifold for different curvature radius

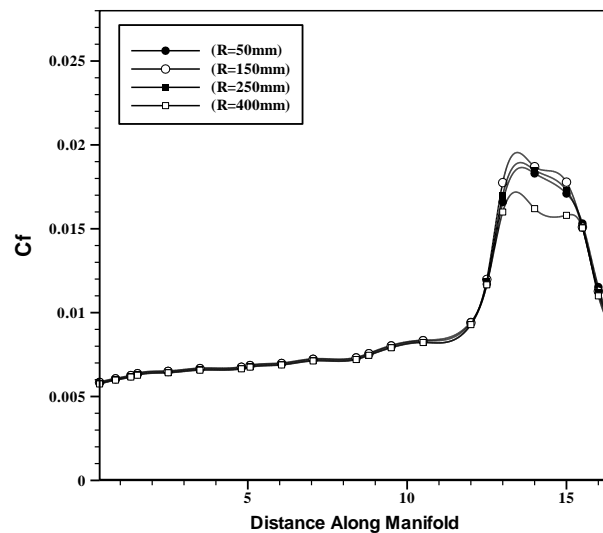


Figure (14) Skin friction distribution at the wall of manifold for different curvature radius

4-4 Influence of the Space between Lateral Pipes:

Figures (15 to 20) shows the effect of an increase in the space between each two consecutive lateral pipes on the properties and behavior of flow inside manifold pipe, where different values of the space have been examined ($l=1.5, 2.5, 4$ m) respectively, with constant area ratio ($A.R=1$). It is well evident that the increase in the space between lateral pipes produces a decrease in the size of lateral recirculation zones, as shown in Fig.(15). Figure (16) show the velocity vector distribution along manifold pipe. From Fig.(17), it is found that the pressure increases along the center-line of the manifold pipe. Figure (18) shows the velocity distribution at centerline of manifold. The flow distribution for ($l=1.5$ m) in Fig.(19) is found 30% from total flow discharged from last lateral and about 10% is discharged from first lateral, while at ($l=4$ m) about 28.5% from total flow is discharged from

last lateral and 10.5% is discharged from first lateral. Then it is found that the disparities in the flow distribution along the manifold pipe decreases as the space increases. **Figure (20)** represents the friction factor distribution along the manifold pipe, whereas the value of friction factor increases as the space between lateral pipes increases.

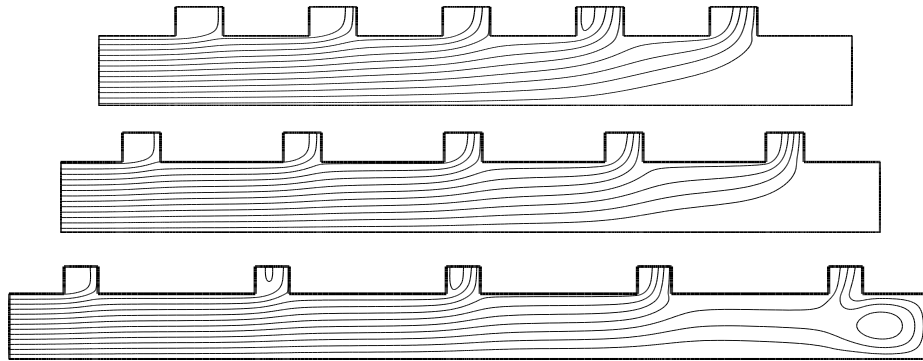


Figure (15) Contours of streamline for (A.R=1), with different space between laterals (l=1.5, 2.5,4 m) respectively

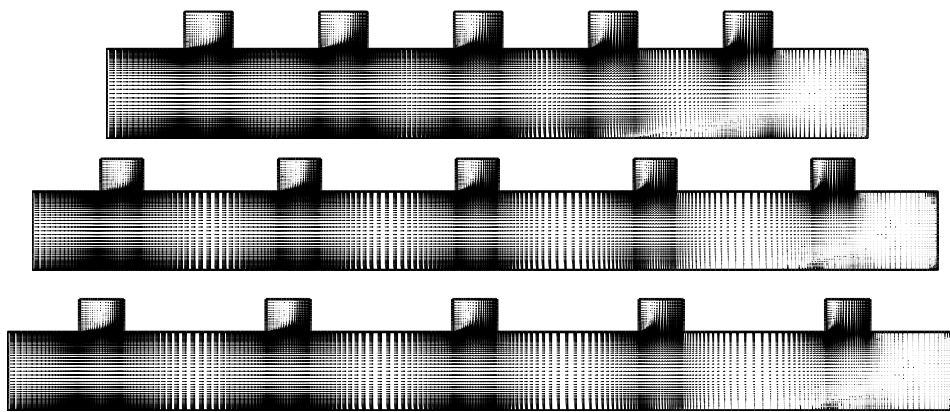


Figure (16) Velocity vectors for manifold of (A.R=1), with different space between laterals (l=1.5, 2.5,4 m) respectively

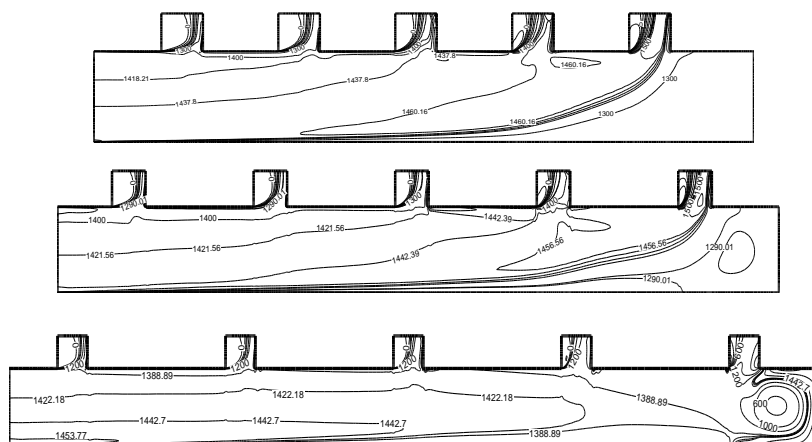


Figure (17) Pressure contours for manifold of (A.R=1), with different space between laterals (l=1.5, 2.5, 4 m) respectively

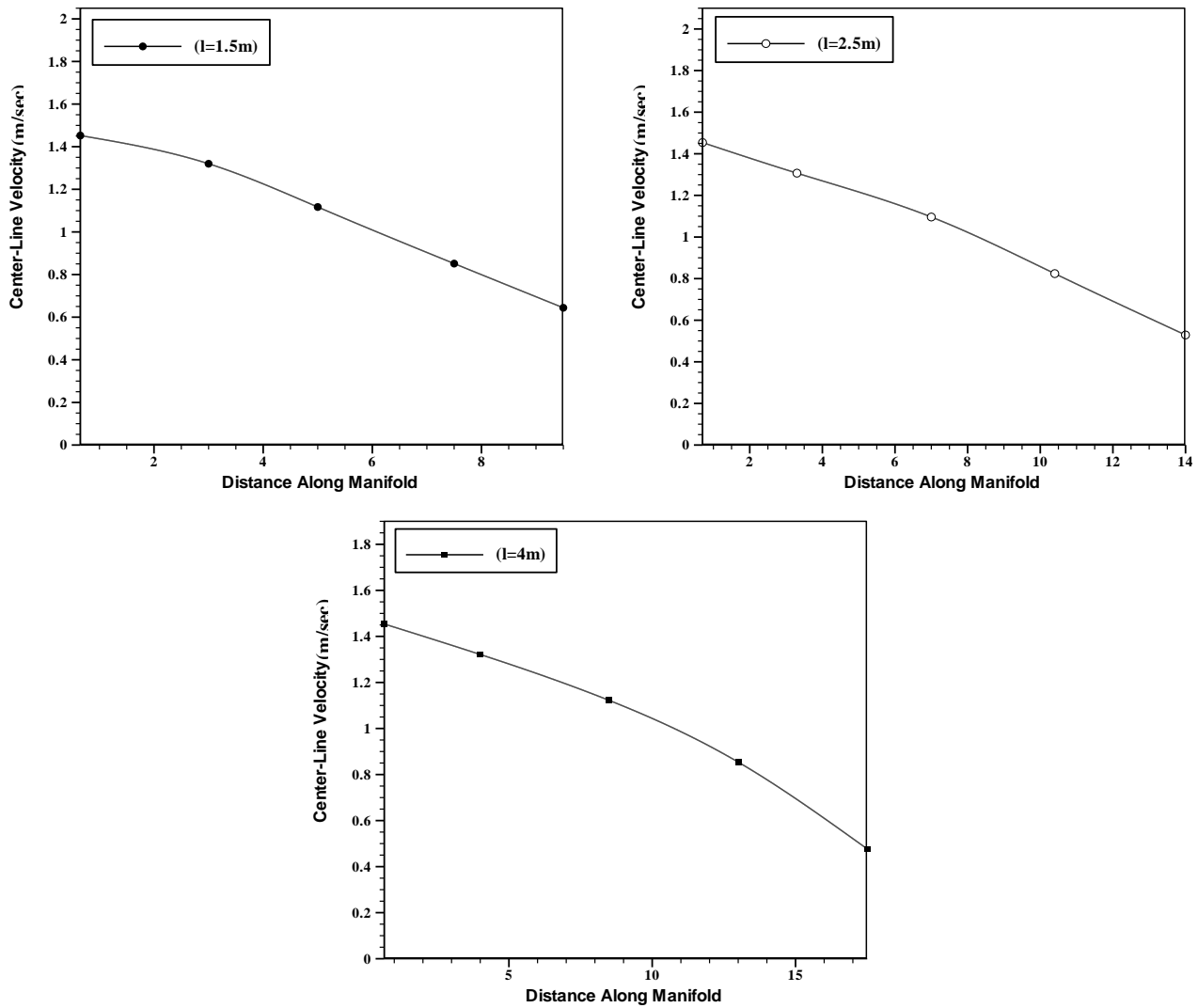


Figure (18) Velocity distribution at center-line of manifold for different space (l=1.5, 2.5,4 m) respectively, (A.R=1), R=0.0001m

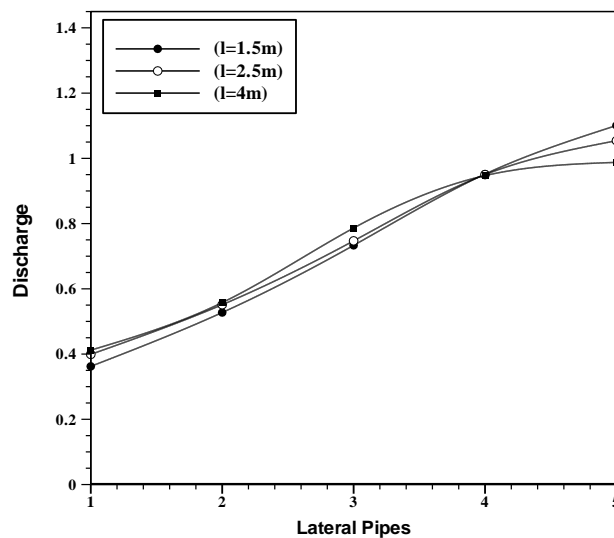


Figure (19) discharge distribution along manifold length for different space (l=1.5, 2.5,4 m) respectively, (A.R=1), R=0.0001m

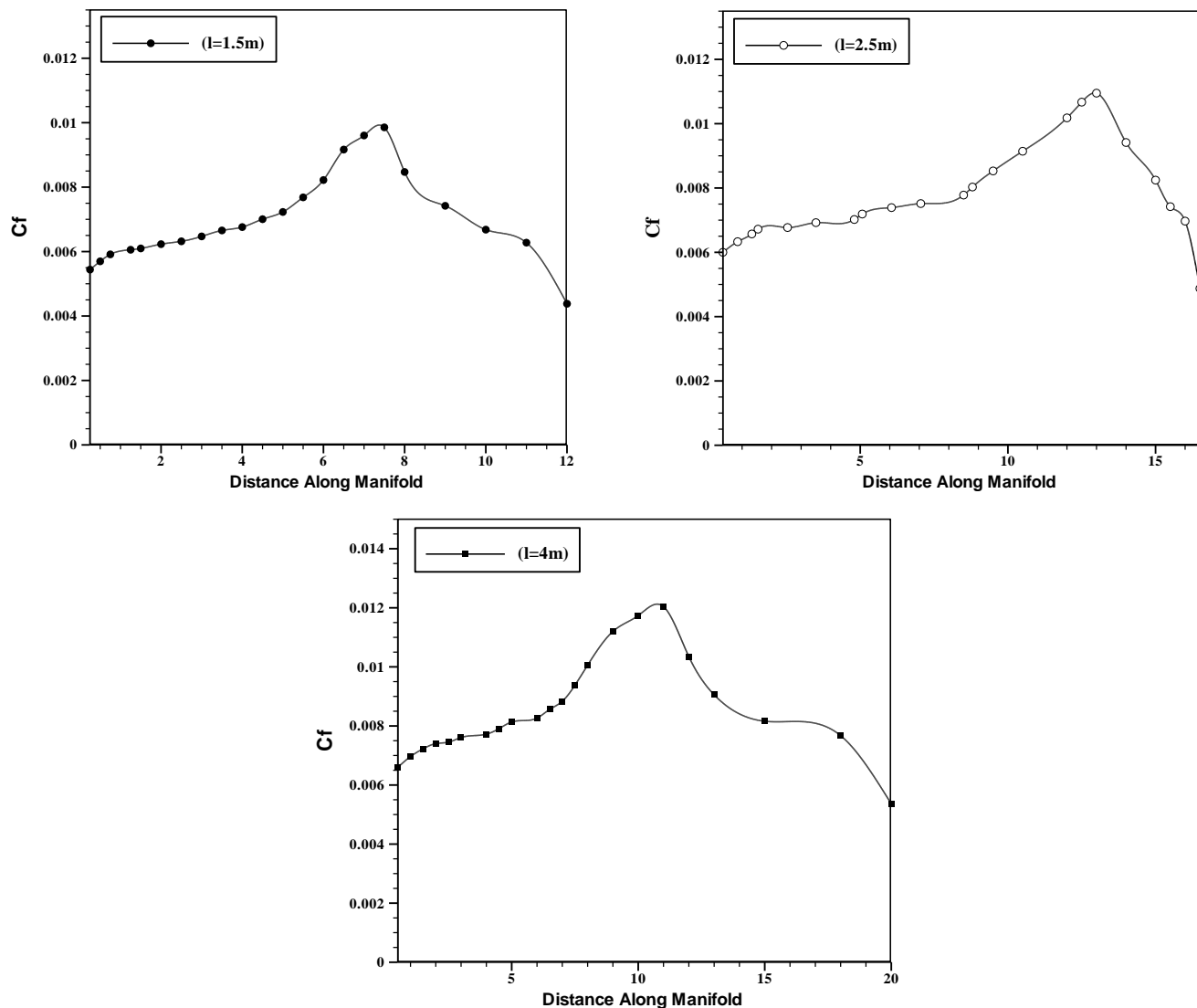


Figure (20) Skin friction distribution at the wall of manifold for different space ($l=1.5, 2.5, 4\text{ m}$) respectively, ($A.R=1$), $R=0.0001\text{m}$

5. Conclusion Remarks

In this work, a successful numerical model based on staggered FVM has been developed for the calculation of two-dimensional incompressible turbulent flow through manifold pipe that divides flow to five consecutive lateral pipes. The influence of several factors on the flow distribution along manifold pipe such as area ratio ($A.R$), curvature radius (R), and space between laterals (l) is clarified. It is concluded that the area ratio has evident influence on flow distribution along manifold pipe, where the percentage of last lateral flow will be decreased, while the percentage of first lateral flow increases as area ratio becomes less than unity ($A.R < 1$), and this condition applies for short manifold ($L/D \leq 10$). For shorter manifold, the discharge distribution along the manifold pipe is far from uniform, even if area ratio is less than unity, as well evident by the change in the configuration of junction point (from sharp-

edged to rounded).As space between each two consecutive laterals is increased, the variation in discharge decrease slowly.

6. References

1. Sullivan, G. R., and Hamilton, M. H., ***“Water Supply: Pumping Stations”***, Technical Manual, Headquarters, Department of the Army, Washington, DC, No.5-813-6, 1992.
2. Keller, J. D., ***“The Manifold Problem”***, Transaction of the ASME, Vol. 71, 1949, pp. 77-85.
3. Bajura, R. A., ***“A Model for Flow Distribution in Manifolds”***, ASME Journal of Engineering for Power, Vol. 93, 1971, pp. 7-12.
4. Hudson, H. E. JR., Uhler, R. B., and Bailey, R. W., ***“Dividing-Flow Manifolds with Squares-Edged Laterals”***, Journal of the Environmental Engineering Division, Vol. 105, 1979, pp. 745-755.
5. Hayes, R. E., Nandakumar, K., and Naser-EL-Din, H., ***“Steady Laminar Flow in A 90° Degree Planar Branch”***, Journal of Computers and Fluids, Vol. 17, No. 4, 1989, pp. 537-553.
6. Neary, V. S., Sotiropoulos, F., and Odgaard, A. J., ***“Three-Dimensional Numerical Model of Lateral-Intake Inflow”***, ASCE Journal of Hydraulic Engineering, Vol. 125, 1999, pp. 126-140.
7. Patankar, S. V., ***“Numerical Heat Transfer and Fluid Flow”***, Hemisphere Publishing Corporation, Taylor and Francis Group, New York, 1980.
8. Versteeg, H. K., and Malalasekera, W., ***“An Introduction of Computational Dynamics-The Finite Volume Method”***, Longman Group Ltd, 1995.
9. Patankar, S. V., and Spalding, D. B., ***“A Calculation Procedure for Heat, Mass and Momentum Transfer in Three-Dimensional Parabolic Flow”***, International Journal of Heat and Mass Transfer, Vol. 15, 1972, pp. 1787.
10. Binne and Partners, ***“Baghdad Drinking Water Network”***, London in Association with Amanat AL-Asima, Baghdad, 1981.

Nomenclature

a_1, a_2, b_1	Coordinate transformation coefficient	
A	Combined diffusion-convection coefficient	
$C_\mu, C_{\varepsilon 1}, C_{\varepsilon 2}$	Constants in the k- ε model	
D	Diffusion term	kg/s
E	Constant used in the low of the wall	
F	Convection term	kg/s
G_k	Production term of kinetic energy	
G_1, G_2	Contravariant velocity components	
J	Determinant of jacobian of transformation	
K	Turbulent kinetic energy	m^2/s^2
L	Characteristic length	m
S	Source term	
T_i	Turbulent intensity	
u, v	Cartesian velocity components	m/s
u_ξ, u_η	Covariant velocity components	
x, y	Cartesian coordinate	M
ΔV	Volume of control unit	m^3
Γ	Diffusion coefficient	
ε	Dissipation rate of turbulent kinetic energy	m^2/s^3
κ	Von Karman constant	
ξ, η	Curvilinear coordinate	
ρ	Density	kg/m^3
τ_w	Wall shear stress	N/m^2
ϕ	Dependent variable	
nb	Abbreviation of neighboring	